IASJ المجلات الاكاديمية العراقية

Tikrit Journal of Pure Science

ISSN: 1813 – 1662 (Print) --- E-ISSN: 2415 – 1726 (Online)

Journal Homepage: http://tjps.tu.edu.iq/index.php/j

Ag/ TiO_2 core/shell NPs synthesized by laser ablation and its antibacterial activity

Maha T. Twafeeq , Falah A-H. Mutlak

Department of physics , College of Science, University of Baghdad, Baghdad, Iraq.

https://doi.org/10.25130/tjps.v26i6.196

ARTICLE INFO.

Article history:

-Received: 24 / 7 / 2021

-Accepted: 26 / 8 / 2021

-Available online: / / 2021

Keywords:

Corresponding Author:

Name: Maha T. Twafeeq

E-mail:

maha_maha0@yahoo.com

Tel:

ABSTRACT

As a consequence of the spread of infectious illnesses caused by numerous harmful bacteria and the development of antibiotic resistance, researchers and pharmaceutical firms are seeking for novel antibacterial medicines. Furthermore, due to their high surface area to volume ratio (SA:V) and unique physical and chemical characteristics, Nano scale materials are emerging as novel antibacterial agents in the contemporary context. In this study, we show how to prepare Ag/ TiO_2 NPs that are pure, stable, and high in concentration. By applying a pulsed laser (Nd:YAG) with different wavelengths of 1064 nm and a length of 532 nm resulting from the second harmonic generation using the KDP crystal, and with a wavelength of 355 nm resulting from the third harmonic generation using the nonlinear crystal KTP to a TiO_2 plate submerged in Ag nanoparticle suspensions previously produced with various energies of 200, 400, 600, 800, and 1000mJ, Ag/ TiO_2 NPs were created. The absorption peak for the sample obtained at 1000 mJ energy is greater than the absorption peak for the sample prepared at 200 mJ, which is attributable to increased nanoparticle concentration. At 440 nm, the remaining peaks are nearly fixed. The absorption rise when the laser wavelength was reduced from 1064 nm to 355 nm and the energy levels were increased from 200 to 1000 mJ, according to our findings. It was discovered that Ag/ TiO_2 has an effect on bacterial activity, with the inhibition area rising as the laser intensity rises. *E.coli* were shown to be more resistant to Ag/TiO_2than *S.aureus*.

Introduction

As a consequence of the growth of infectious illnesses caused by numerous harmful bacteria and the development of antibiotic resistance, pharmaceutical firms and researchers are always seeking for new antibacterial medications [1,2]. Nano scale materials have emerged as new antibacterial agents [3]. Professor Norio Taniguchi of Tokyo Science University coined the word "nanotechnology" in 1974 to describe the precise manufacture of nanoscale materials. [4]. Professor Richard P. Feynman, a physicist, introduced the notion of nanotechnology in his speech. At the Bottom, there's lots of space [5]. Bio nanotechnology is the combination of biotechnology and nanotechnology for the development of biosynthetic and environmentally friendly nanomaterial synthesis technology. Nanoparticles are atom clusters that range in size from 1 to 100 nanometers. Nano is a Greek term that means "very tiny" and is equivalent with the word "dwarf." Nanoparticles are gaining popularity in the twenty-first century because of their well-defined chemical, optical, and mechanical characteristics. Metallic nanoparticles are the most promising because of their antibacterial characteristics, which are gaining researchers' interest due to the rising microbial resistance to metal ions and antibiotics, as well as the creation of resistant strains [6]. Copper, zinc, and titanium are examples of nanomaterial's [7]. Gold, magnesium [8], alginate [9] Silver nanoparticles have shown to be the most effective because they have high antibacterial effectiveness against bacteria, viruses, and other eukaryotic microorganisms. Exposure to silver nanoparticles, which are employed as medication disinfectants, can cause agyrosis and argyria, as well as being harmful to mammalian cells [6].

Silver ion or metallic silver, as well as silver nanoparticles, can be used in medicine for burn treatment, dental materials, coating stainless steel materials, textile fabrics, water treatment, sunscreen lotions, and other applications, according to the current study, and are low in toxicity to human cells, have high thermal stability, and have low volatility [10]. Because of their unique characteristics, nanostructured and nanophasic materials have been widely investigated, extending the range of their applicability in several sectors. The influence of nanostructure on the characteristics of high surface area materials is becoming increasingly important in terms of understanding, developing, and enhancing materials for a variety of applications [11]. Metal oxides are the most frequent, diversified, and perhaps the richest class of materials in terms of physical, chemical, and structural characteristics among the major classes of materials. Furthermore, due to their tiny size and larger number of surface atoms, oxide nanoparticles might show unique physical and chemical characteristics [12]. Because of its potential applications in catalysis/photo catalysis, self-cleaning surface coatings, photovoltaic applications, and the removal of heavy metal ions from solutions for detoxification and the oxidation of toxic organic contaminants in water to carbon dioxide, Nano crystalline titania (TiO_2) is becoming increasingly important [13]. TiO_2 has a wide range of uses due to characteristics such as chemical inertness, non-toxicity, and stability across a wide pH range under irradiation [14, 15]. Silver has been used for the treatment of burns and chronic wounds for millennia. Silver was used to produce drinkable water as early as 1000 B.C. [16,17]. Following the introduction of penicillin in the 1940s, the use of silver for the treatment of bacterial infections declined [18,19,20]. When Moyer introduced the use of 0.5 percent silver nitrate for the treatment of burns in the 1960s, silver was once again in the spotlight. He claims that this solution has antibacterial properties against Staphylococcus *S.aureus*, Pseudomonas aeruginosa, and Escherichia coli while not interfering with epidermal growth [21, 22]. Silver sulfadazine cream was created in 1968 by combining silver nitrate with sulfonamide and was used to treat burns as a broad-spectrum antibacterial agent. *E. coli*, *S. aureus*, Klebsiella sp., and Pseudomonas sp. are all susceptible to silver sulfadazine. It has antifungal and antiviral properties as well [23]. Clinicians have recently reverted to silver wound dressings with various levels of silver due to the rise of antibiotic-resistant bacteria and limits in the use of antibiotics [24,25].

Experimental Setup

Figure 1 shows the experimental setup for laser ablation of an Ag target immersed in (5 ml) of pure distal water, where the laser wavelength is (1064, 532, 355) nm and the pulse rate is (1 Hz) with (700) pulses for several energies (200, 400, 600, 800, 1000) mJ, and the Ag target is placed in the bottom of a glass container filled with pure water, then we put the glass container on a metal disk above a small circular holder moving 2 cycles per minute to distribute the pulses across the entire surface of the Ag target, then we took water containing Ag nanoparticles pre-prepared by the energies male above, then we immersed Ti plate in Ag nanoparticle to prepare Ag/TiO_2 for laser with different wavelengths of 1064 nm and a length of 532 nm resulting from the second harmonic generation using the KDP crystal, and with a wavelength of 355 nm resulting from the third harmonic generation using the nonlinear crystal KTP.

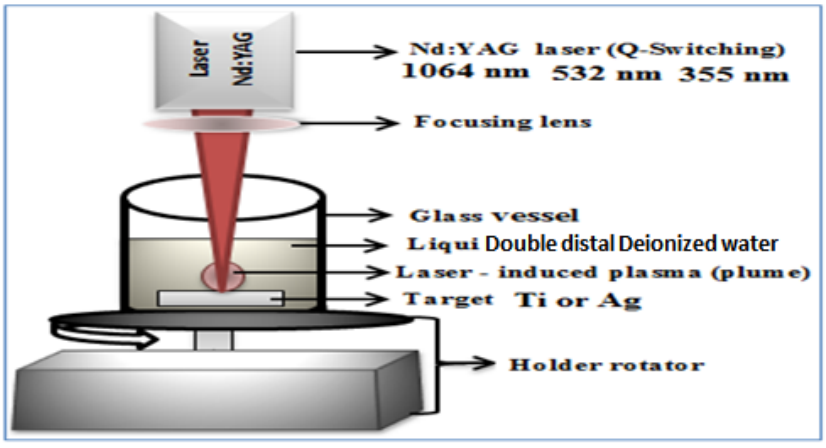

Fig. 1: Schematic diagram of PLAL

In this work a pulsed Nd: YAG laser system has been utilized, the information about the method can be presented in table 1.

Table 1: Show the information about PLAL method.

Parameter	Details
Wavelength of Laser beam	1064 nm, 532 nm, 355 nm
Number of laser pulses	700 pulse
Laser Energy	200 mJ, 400 mJ, 600 mJ, 800 mJ, 1 J
Beam diameter of Laser	4.3 mm
Repetition rate	1 Hz
Pulse duration	9 ns
The distance between the target and lens	12 cm
Cell	Glass vessel
Liquid	Double distal Deionized water
Target	Ti and Ag with purity 99.9%

Results and Discussion

Figure 2 illustrates the absorbance spectra of Ag/ TiO_2 NPs produced at 1064 nm. PLAL with 200mJ, 400mJ, 600mJ, 800mJ, and 1000mJ laser energy. The absorption peaks in the visible region indicate the production of metal NPs, while the confinement in the Nano-scale has been demonstrated by a red shift in the Plasmon absorption peak relative to TiO_2 bulk. A Semi symmetric absorption band centered at 440-447 nm can be seen in the SPE spectra of the silver nanoparticles solution.

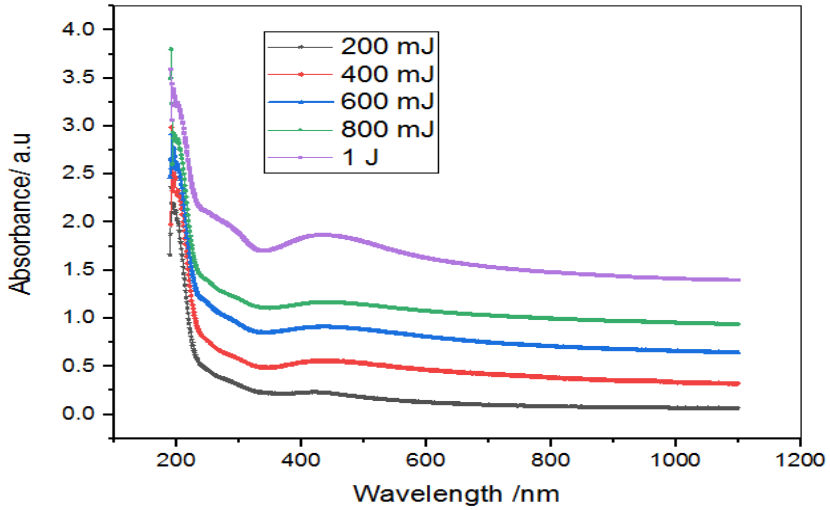

Fig. 2: Absorption spectra of Ag/TiO_2 NPs for wavelength (1064) nm

Figure 3 illustrates the impact of wavelength 532 nm on the absorption spectra of Ag/ TiO_2 NPs, demonstrating that 1000 mJ is the optimum energy for enhancing absorbance. According to Beer-lambert low, this may be read as an increase in TiO_2 concentration. Figure 4 shows the absorption spectra of Ag/ TiO_2 NPs produced for laser at 355 nm wavelength, exhibited a noticeable increase in the absorbance of Ag/ TiO_2 NPs, as well as a shift to the long wavelength visible light region, indicating that the energy band gap of TiO_2 is being decreased by Ag NPs.

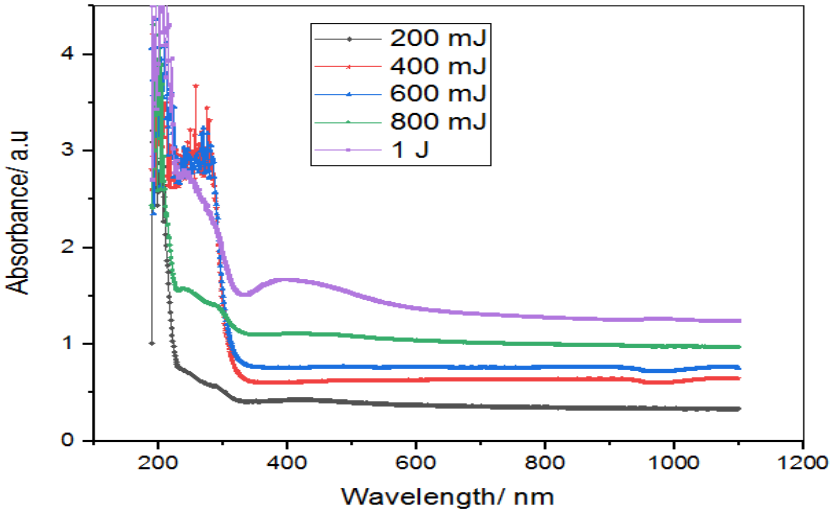

Fig. 3: Absorption spectra of Ag/ TiO_2 NPs for wavelength (532) nm

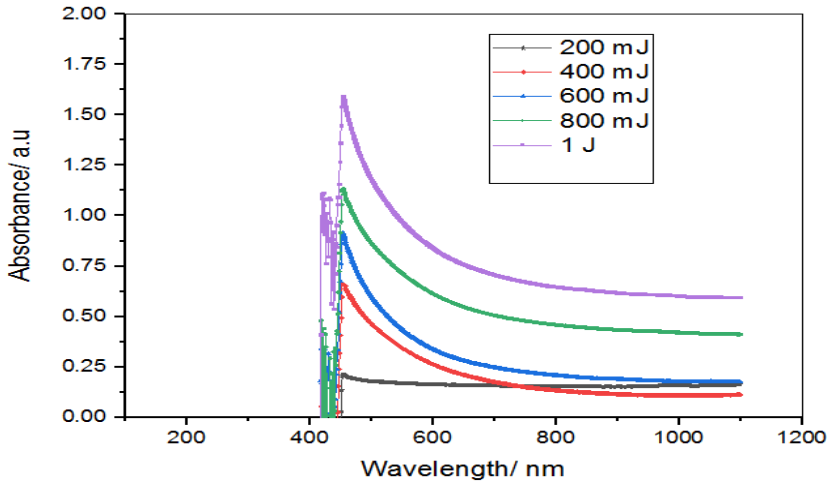

Fig. 4: Absorption spectra of Ag/TiO_2 NPs for wavelength (355) nm

The Structure Properties of Ag/ TiO_2 NPs we used XRD to construct the crystal structure of Ag/TiO_2. As shown in Figure (5). Samples were prepared by the drop-casting of Ag/TiO_2 NPs on a silicon surface. The sample diffraction pattern was indexed, and Miller Indices (hkl) were assigned to each peak. The peaks at 38.2°,44.2°, 64.6°,and 77.4° might be indexed as (111), (200), (220), and (311) lattice planes regarding Ag or TiO_2 NPs. As TiO_2 and Ag have been comparable lattice parameters, also complete miscibility for composition range, such lattice planes have indicated in core-shell structures and cubic Ag/TiO_2 alloy. Also, lattice plane of [111] has been indicated, since it comes with high free energy and fast grow rate. All these patterns were analyzed by the Riveted method inside the XRD instrument, using the refinement system for every pattern, and determined FWHM values of XRD peaks, taking into account the instrumentation contribution in the broadening of those peaks. For XRD investigations, a portion of the solid matrix was dried and maintained hard. Diffraction pattern corresponding to impurities were found to be absent. This proved that pure TiO_2 NPs were synthesized.

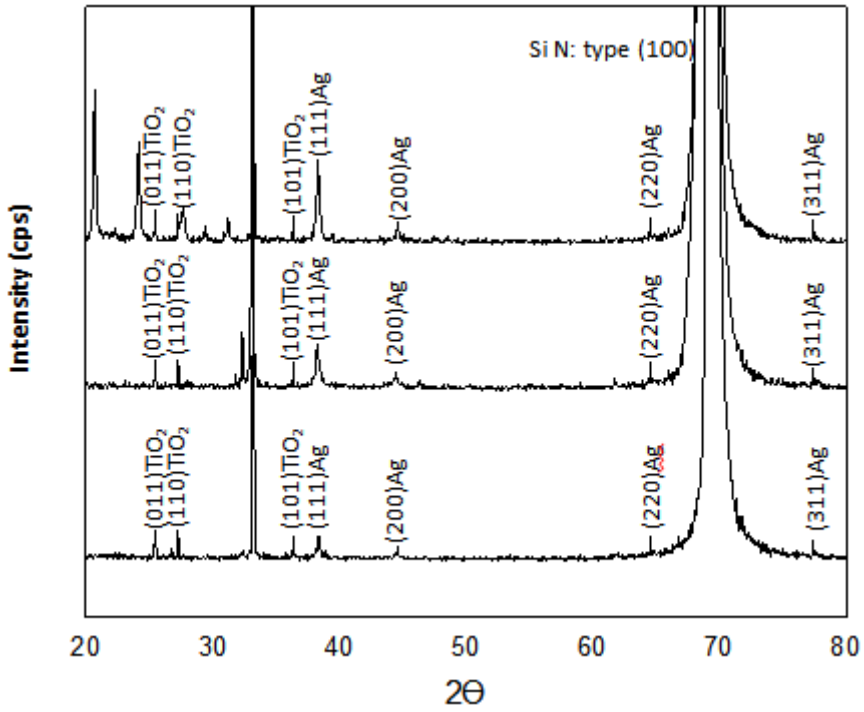

Fig. 5: X-ray diffraction pattern of Ag/Tio2 NPs in different wavelength 1064nm, 532nm, 355nm

Table 2: XRD peaks of Ag/ TiO_2 NPs.

2θ(Deg.)	FWHM (Deg.)	dhkl Exp.(Å)	G.S(nm)	dhkl Std. (Å)	hkl	Phase	card No.
38.2	0.75112	2.3577	9.4	2.3500	(111)	Cub. Au	96-901-2431
44.2	26.59906	2.0536	5.6	2.0352	(200)	Cub. Au	96-901-2431
64.6	16.11918	1.4352	15.7	1.4391	(220)	Cub. Au	96-901-2431
77.4	12.37843	1.2280	13.0	1.2273	(311)	Cub. Au	96-901-2431
25.3	0.5091	3.5055	16.0	3.5372	(011)	Anatase	96-900-8217
27.6	0.5191	3.2266	15.8	3.2483	(110)	Rutil	96-900-9084
36.4	0.5285	2.4652	15.8	2.4871	(101)	Rutil	96-900-9084

Surface imaging and elemental analyses of the samples were carried out using scanning electron microscopy (SEM). Figures (6),(7),(8),(9),(10),(11) show (SEM-EDS) images for Ag/TiO_2 NPs by pulsed laser ablation in DDW with laser energy at 1000mJ wavelength 1064 nm and 532 nm and 355 nm , respectively. Ag/TiO_2 NPs deposited on a silicon substrate. The samples were dropped onto a silicon wafer and investigated by field emission scanning electron microscopy (FE-SEM) in order to study particle or grain size, nanoparticles shapes, and surface morphology. The magnification power was 100kx for all samples.

The Ag/TiO_2 core/shell nanoparticles prepared with 1000mJ and wavelength 1064nm have spherical shape and diameters were average 20-33 nm. The Ag/TiO_2 core/shell nanoparticles prepared with 1000mJ and wavelength 532nm have spherical shape and diameters were approximately 17-35 nm. The Ag/TiO_2 core/shell nanoparticles prepared with 1000mJ and wavelength 355nm have spherical shape and diameters were approximately 17-35 nm.

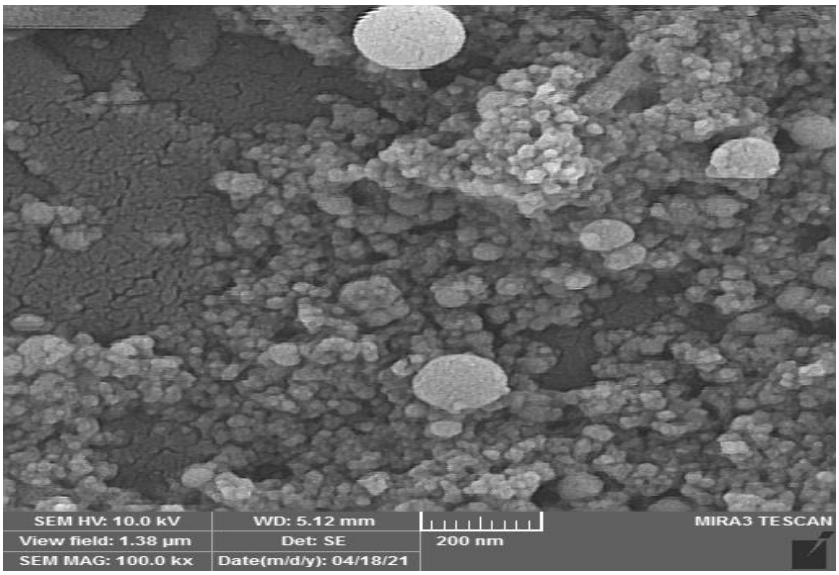

Fig. 6: SEM image for Ag/TiO_2 NPs synthesized by 1064nm

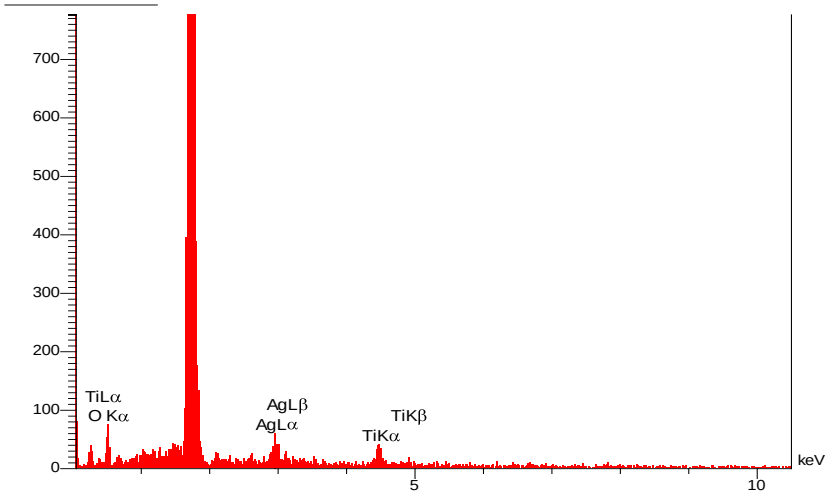

Fig. 7: SEM-EDS images for Ag/TiO_2 NPs synthesized by 1064nm

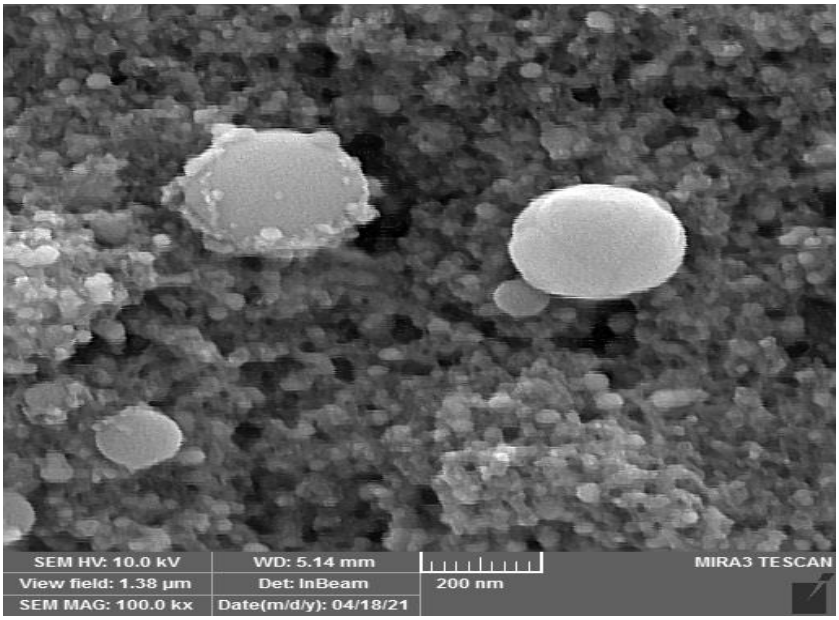

Fig. 8: SEM image for Ag/TiO_2 NPs synthesized by 532nm

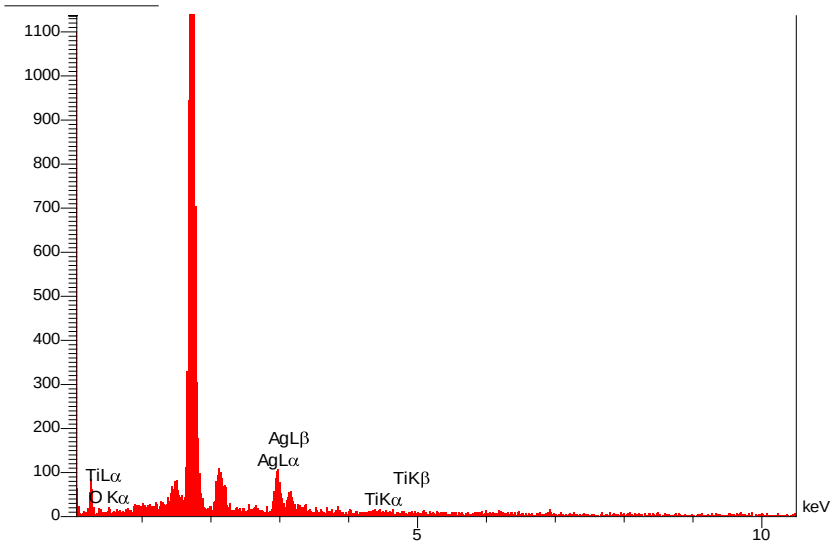

Fig. 9: SEM-EDS images for Ag/TiO_2 NPs synthesized by 532nm

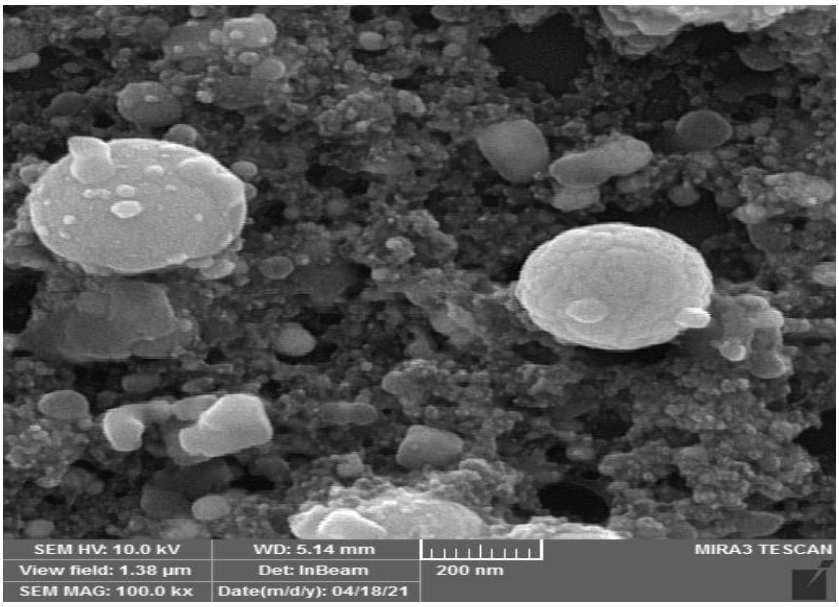

Fig. 10: SEM image for Ag/TiO_2 NPs synthesized by 355nm

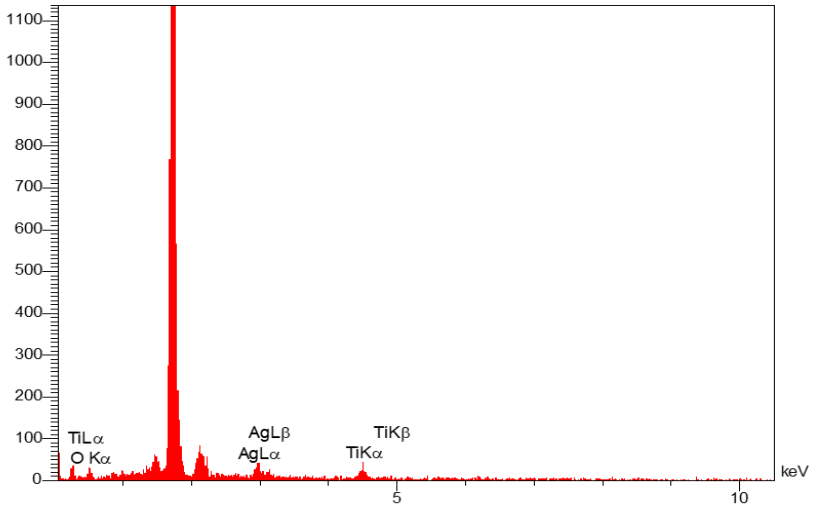

Fig. 11: SEM image for Ag/TiO_2 NPs synthesized by 355nm

Antibacterial activity of Nanoparticles

S.aureus and *E. coli* were used to test the nanoparticles' antibacterial efficacy. After exposing the organisms to various doses of nanoparticles, the zones of inhibition were quantified and plotted (12, 13, 14). The antibacterial activity of Ag/ TiO_2 NPs was investigated using different laser energy on the bacterium *S.aureus* and *E.coli* (200,400,600,800and 1000 mJ). Figures show the width of the zone of inhibition of Ag/ TiO_2 NPs on bacteria strains, with Ag/ TiO_2 NPs having a greater impact on E. coli and *S.aureus*. As the concentration of Ag/ TiO_2 NPs was raised, the inhibition zone grew considerably. *E.coli* was less susceptible to Ag/ TiO_2 NPs than *S.aureus*. *E. coli* is a Gram-negative bacterium that is less susceptible to antimicrobials than Gram-positive bacteria like *S.aureus* because it is more resistant to lipophilic and amphiphilic inhibitors, such as dyes, detergents, free fatty acids, antibiotics, and chemotherapeutic agents, than Gram-positive bacteria like *S.aureus*. It's possible that the existence of the outer membrane is to blame. The low fluidity of the lipopolysaccharide layer hindered the rate of Tran's membrane diffusion of lipophilic solutes, while the pore channels delayed the penetration of tiny hydrophilic solutes [26]. The concentration and size of the nanoparticles, which play a key role in the antibacterial process, are also essential variables. The antibacterial action of Ag/ TiO_2 NPs against both gram-positive and gram-negative bacteria is dependent on the Ag NP concentration. The catalytic and antibacterial mechanisms of Ag NPs have been shown to increase when the average size decreases. Nanoparticles have a wide surface area to come into touch with bacterial cells, implying that they will have a higher proportion of engagement than larger particles. Nanoparticles smaller than 10nm interact with bacteria, causing electrical effects that increase nanoparticle reactivity. The antibacterial effectiveness of nanoparticles is also influenced by their form, as evidenced by research into the suppression of bacterial growth by differently shaped nanoparticles. The direct contact of Ag/ TiO_2 nanoparticles with bacteria cells can result in damaging consequences such as cell membrane penetration and cell function impairment. Increased intracellular ROS production may be another route of antibacterial action, since the high surface to volume ratio provides more efficient mechanisms for improved antibacterial activity. According to Azam et al., this is a reasonable explanation [27]. The antibacterial action of the Ag/ TiO_2 NPs was achieved in two stages. They decreased the metabolic process by changing the membrane potential and decreasing adenosine triphosphate (ATP) synthase activity. Second, they rejected the ribosome's component for tRNA binding, thus dismantling its biological process. They were also shown to be less harmful to mammalian cells [28] Furthermore, TiO2 and ZnO nanoparticles have shown topromote the antibacterial activity of 8 mm against bacteria *S. aureus* and *E. coli* [29]. Several studies suggested the possible mechanisms involving the interaction of nanomaterial's with biological molecules. It is believed that microorganisms carry a negative charge while metal oxides carry a positive charge. This creates an "electromagnetic" attraction between the microbe and treated surface. Once the contact is made, the microbe is oxidized and dies instantly [30,31].

Prepare the media

Medium Brain Heart Infusion agar

40 g of the dried medium was dissolved in 1 liter of distilled water and placed in an autoclave for 15 minutes at a temperature of 121 °C to sterilize the medium from blackboards and other microorganisms and then poured into sterilized Petri dishes after cooling to 45 °C And keep it in the fridge until use.

Middle Muller Hinton agar

40 g of the dried medium was dissolved in 1 liter of distilled water and placed in an autoclave for 15 minutes at a temperature of 121 °C and 1 bar per square inch to sterilize the medium from blackboards and other microorganisms and then poured into Petri dishes. Sterilized after cooling to 45°C and kept in the refrigerator until use.

Allergy test

The sensitivity of isolates of pathogenic bacteria (*E.coli* and *S.aureus*) to 5 different concentrations of nanomaterials was tested and the well diffusion method was used. The pathogenic bacteria were grown on solid brain and heart infusion agar and incubated at 37 °C. M for 18-24 hours and after the incubation period, 1-3 young and pure colonies are transferred to test tubes containing 5 ml of normal saline to form a bacterial suspension and growth comparison with MacFarland tube which gives a number of cells 1.5 x 108 CFU / ml Then 0.1 ml of the bacterial suspension was transferred and spread homogeneously on the solid Muller Hinton agar medium. The medium was perforated by a cork drill with 6 holes for each dish (dish size 200 mm square) at a distance of 30 mm from one hole and another and 30 mm from the edge of the dish . 100 µl of nanomaterial was placed in each hole and 100 µl distilled water control solution was placed in one hole in each dish and the inhibition areas were compared in millimeters for each concentration of bacterial isolates.

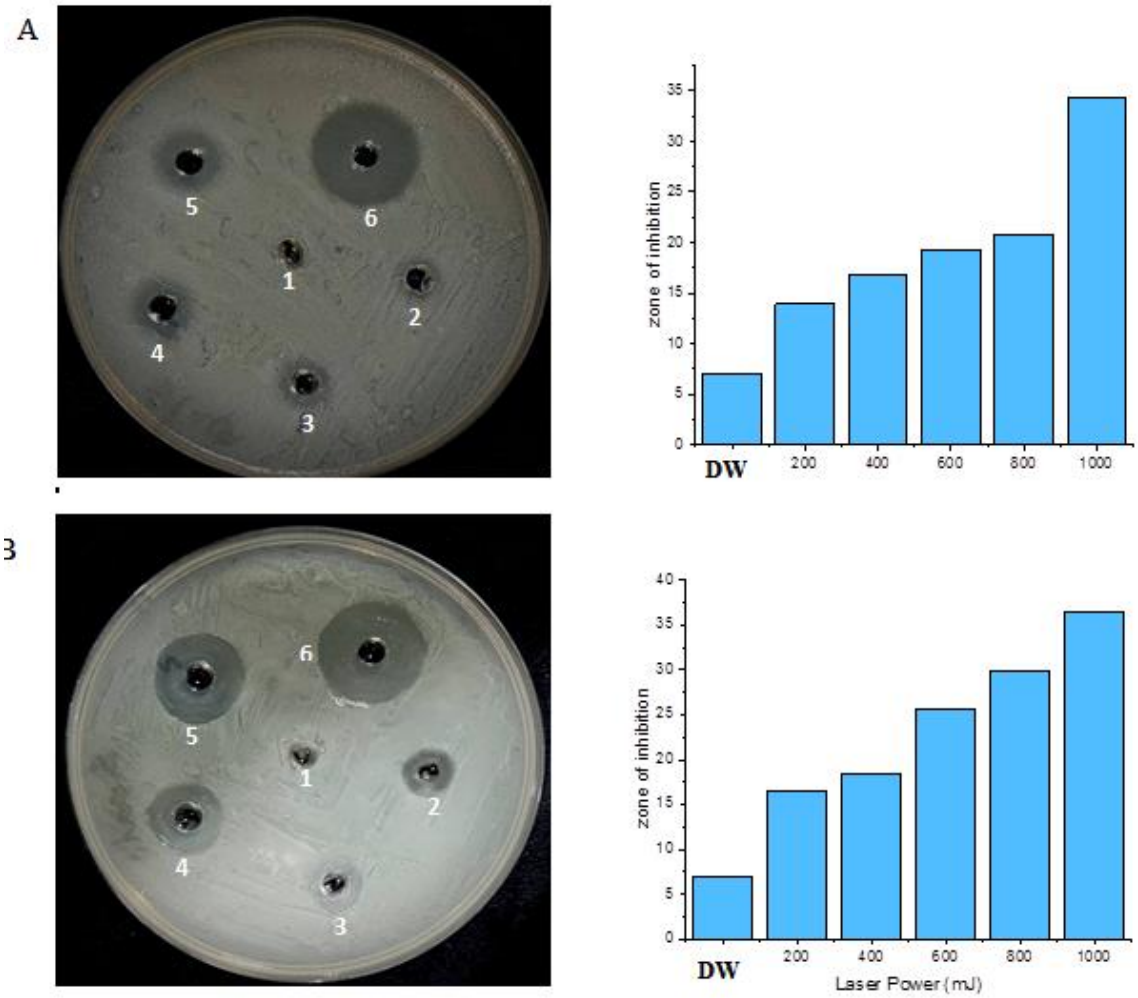

Fig. 12: Anti-bacterial activity of nanoparticles against A: *E.coli* and B: *S.aureus*.1: Negative control, 2:200mJ, 3: 400mJ, 4: 600mJ, 5: 800mJ, 6: 1000mJ, with wavelength 1064 nm

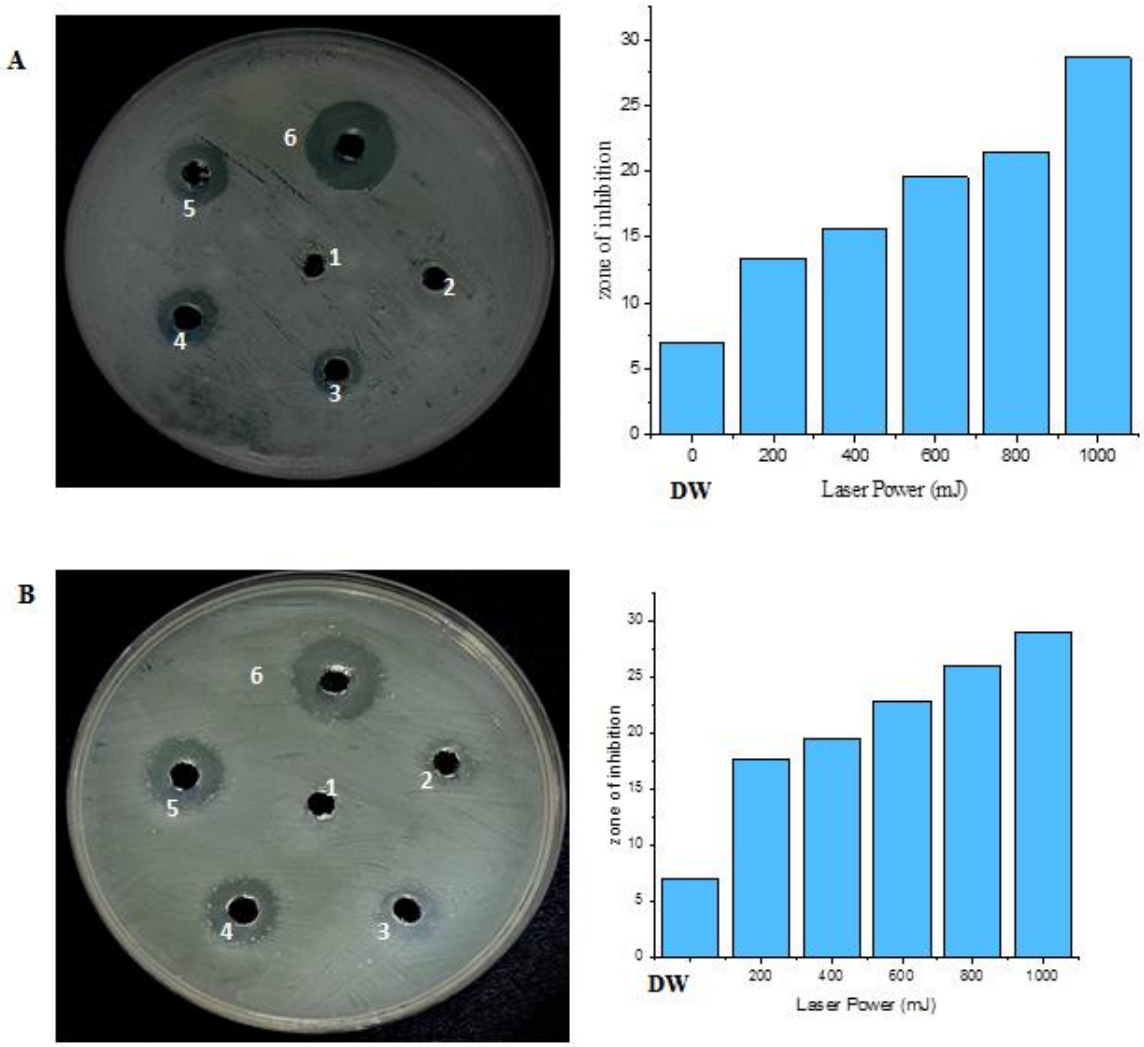

Fig. 13: Anti-bacterial activity of nanoparticles against A: *E.coli* and B: *S.aureus*.1: Negative control, 2:200mJ, 3: 400mJ, 4: 600mJ, 5: 800mJ, 6: 1000mJ, with wavelength 532 nm

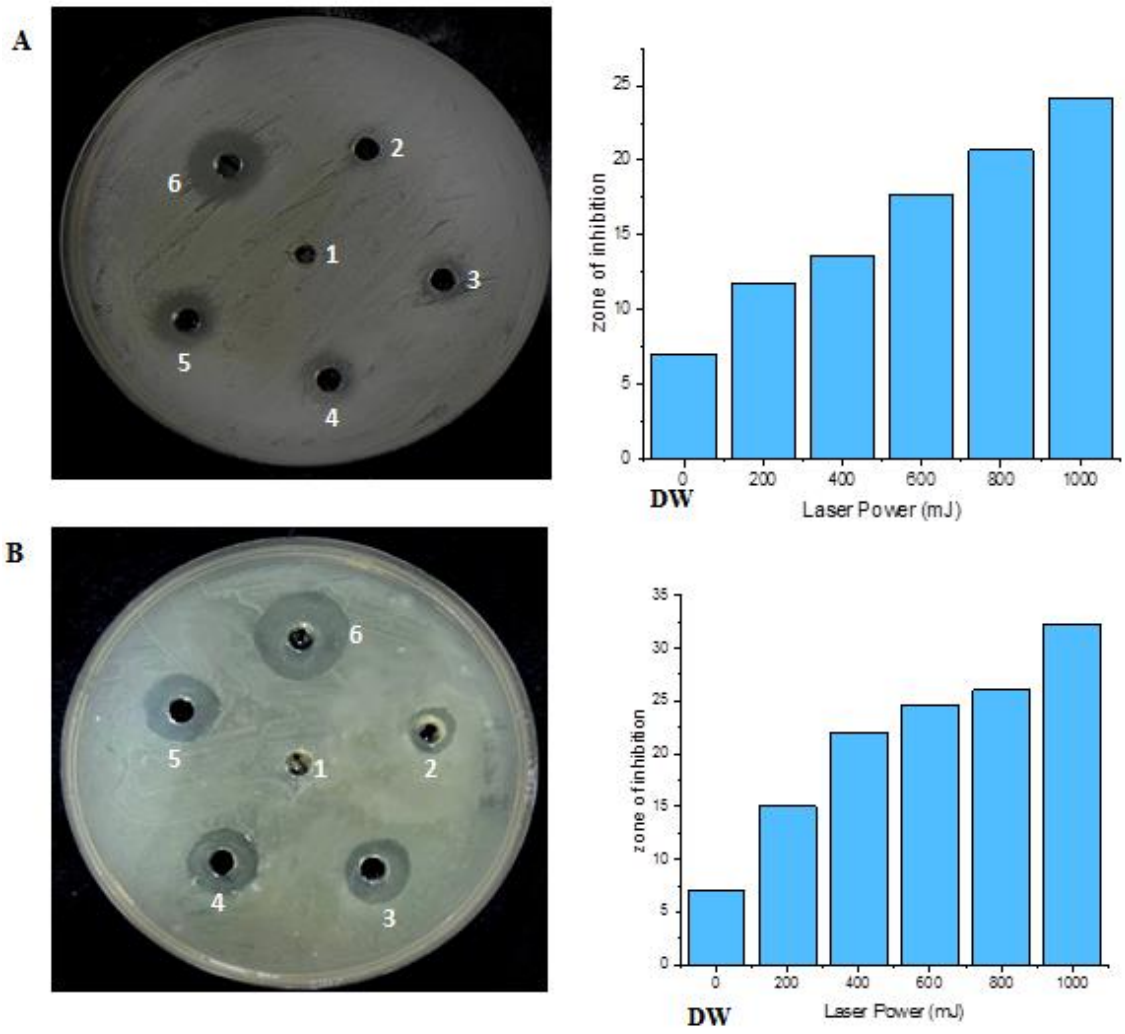

Fig. 14: Anti-bacterial activity of nanoparticles against A: *E.coli* and B: *S.aureus*.1: Negative control, 2:200mJ, 3: 400mJ, 4: 600mJ, 5: 800mJ, 6: 1000mJ, with wavelength 355 nm

Table 3: zone of inhibition of Ag/ TiO_2 NPs synthesis by PLAL at wavelength 1064 nm and different energy.

wavelength 1064 nm			
E.coli		***S.aureus***	
Energy (mJ)	**zone of inhibition (mm)**	**Energy (mJ)**	**zone of inhibition (mm)**
200	13	200	16
400	16	400	18
600	19	600	25
800	20	800	29
1000	34	1000	36

Table 4: zone of inhibition of Ag/ TiO_2 NPs synthesis by PLAL at wavelength 532 nm and different energy.

wavelength 532 nm			
E.coli		***S.aureus***	
Energy (mJ)	**zone of inhibition (mm)**	**Energy (mJ)**	**zone of inhibition (mm)**
200	13	200	17
400	15	400	19
600	19	600	22
800	21	800	25
1000	28	1000	29

Table 5: zone of inhibition of Ag/ TiO_2 NPs synthesis by PLAL at wavelength 355 nm and different energy.

wavelength 355 nm			
E.coli		*S.aureus*	
Energy (mJ)	zone of inhibition (mm)	Energy (mJ)	zone of inhibition (mm)
200	11	200	15
400	13	400	22
600	17	600	24
800	20	800	26
1000	24	1000	32

Conclusions

The Nd:YAG laser ablation was used to bind the smaller Ag particles to the larger TiO_2 particles, and it was a good way to combine two different nanoparticles. It was discovered that the activity of the nanoparticles is directly proportional to their concentration, while the sizes of the NPs are affected by the laser wavelength in the nanosecond laser. The lower the diameters, the shorter the laser wavelengths, therefore nanoparticles with a wavelength of 355 nm are smaller than nanoparticles with wavelengths of 532 nm and 1064 nm. It was discovered that Ag/ TiO_2 has an effect on bacterial activity, with the inhibition area rising as the laser intensity rises. *E.coli* were shown to be more resistant to Ag/ TiO_2 than *S.aureus* , Ag/TiO2 NPs showed an inhibition zone of 11- 34mm against *E. coli*, while 15 - 36mm was observed against *S. aureus.*

References

[1] Morones JR, Elechiguerra JL, Camacho A, Ramirez JT. The bactericidal effect of silver nanoparticles. Nanotechnology 2005;16:2346–53.

[2] Kim JS, Kuk E, Yu KN, Kim JH, Park SJ, Lee HJ, et al. Antimicrobial effects of silver nanoparticles. Nanomed Nanotechnol Biol Med 2007;3:95-101.

[3] Albrecht MA, Evan CW, Raston CL. Green chemistry and the health implications of nanoparticles. Green Chem 2006;8:417–32.

[4] Taniguchi N. On the Basic Concept of Nano-Technology. Proc. Intl. Conf. Prod. Eng. Tokyo, Part II. Japan Society of Precision Engineering; 1974.

[5] Feynman R. Lecture at the California Institute of Technology; 1959. December 29. Fox CL, Modak SM. Mechanism of silver sulfadiazine action on burn wound infections. Antimicrob Agents Chemother 1974;5(6):582–8.

[6] Gong P, Li H, He X, Wang K, Hu J, Tan W, et al. Preparation and antibacterial activity of Fe3O4@Ag nanoparticles. Nanotechnology 2007;18:604–11.

[7] Raimondi F, Scherer GG, Kotz R, Wokaun A. Nanoparticles in energy technology: examples from electochemistry and catalysis. Angew. Chem., Int. Ed. 2005;44:2190–209.

[8] Gu H, Ho PL, Tong E, Wang L, Xu B. Presenting vancomycin on nanoparticles to enhance antimicrobial activities. Nano Lett 2003;3(9):1261–3.

[9] Ahmad Z, Pandey R, Sharma S, Khuller GK. Alginate nanoparticles as antituberculosis drug carriers: formulation development, pharmacokinetics and therapeutic potential. Ind J Chest Dis Allied Sci 2005;48:171–6.

[10] Duran N, Marcarto PD, De Souza GIH, Alves OL, Esposito E. Antibacterial effect of silver nanoparticles produced by fungal process on textile fabrics and their effluent treatment. J Biomed Nanotechnol 2007;3:203–8.

[11] Koch, C.C., 2006. Nanostructured Materials: Processing, Properties and Potential Applications, second ed., Noyes publications, New York.

[12] Rodríguez, J.A., Fernández-García, M., 2007. Synthesis, Properties and Applications of Oxide Nanomaterials. John Wiley & sons, New Jersey.

[13] Fujishima, A., Zhang, X, 2006.Titanium Dioxide Photocatalysis: Present Situation and Future Approaches. Comptes Rendus Chimie 9, 750-760.

[14] Sharad, S., Mohan, C., Giridhar, M., 2012. Visible light photocatalytic inactivation of Escherichia coliwith combustion synthesized TiO2. Chemical Engineering Journal 189-190, 101-107.

[15] Fujishima, A., Rao, TN., Tryk, D.A., 2000. Titanium dioxide photocatalysis. Journal of Photochemistry and Photobiology C: Ph otochemistry Reviews 1, 1-21.

[16] Richard JW, Spencer BA, McCoy LF, Carina E, Washington J, Edgar P, et al. Acticoat versus silverlon: the truth. J Burns Surg Wound Care 2002;1:11–20.

[17] Castellano JJ, Shafii SM, Ko F, Donate G, Wright TE, Mannari RJ, et al. Comparative evaluation of silver-containing antimicrobial dressings and drugs. Int Wound J 2007;4(2):114–22.

[18] Hugo WB, Russell AD. Types of antimicrobial agents. In: Principles and practice of disinfection, preservation and sterilization. Oxford, UK: Blackwell Scientific Publications; 1982. p. 106. 8.

[19] Demling RH, DeSanti L. Effects of silver on wound management. Wounds 2001;13:4.

[20] Chopra I. The increasing use of silver-based products as antimicrobial agents: a useful development or a cause for concern? J Antimicrob Chemother 2007;59:587–90.

[21] Moyer CA, Brentano L, Gravens DL, Margraf HW, Monafo WW. Treatment of large human burns

with 0.5% silver nitrate solution. Arch Surg 1965;90:812–67.
[22] Bellinger CG, Conway H. Effects of silver nitrate and sulfamylon on epithelial regeneration. Plast Reconstr Surg 1970;45:582–5.
[23] Fox CL, Modak SM. Mechanism of silver sulfadiazine action on burn wound infections. Antimicrob Agents Chemother 1974;5(6):582–8.
[24] Gemmell CG, Edwards DI, Frainse AP. Guidelines for the prophylaxis and treatment of methicillin-resistant Staphylococcus aureus (MRSA) infections in the UK. J Antimicrob Chemother 2006;57:589–608.
[25] Chopra I. The increasing use of silver-based products as antimicrobial agents: a useful development or a cause for concern? J Antimicrob Chemother 2007;59:587–90.
[26] V. Amendola & M. Meneghetti (Laser ablation synthesis in solution and size manipulation of noble metal nanoparticles) Physical Chemistry Chemical Physics, Vol.11 (2009) pp.3805-3821.
[27] Patterson, A. "The Scherrer Formula for X-Ray Particle Size Determination". *Phys. Rev*. 56 (10): 978–982 , (1939).
[28] Murphy, Douglas B. "Fundamentals of Light Microscopy and Electronic Imaging". New York: John Wiley & Sons. (2002).
[29] Nguyen, V.T.; Vu, V.T.; Nguyen, T.A.; Tran, V.K.; Nguyen-Tri, P. Antibacterial activity of TiO2 - and ZnO-decorated with silver nanoparticles. J. Compos. Sci. 2019, 3, 61.
[30] Savi, G.D.; Trombin, A.C.; da Silva Generoso, J.; Barichello, T.; Possato, J.C.; Ronconi, J.V.V.; da Silva Paula, M.M. Antibacterial acivity of gold and silver nanoparticles impregnated with antimicrobial agents. Saúde Pesqui. 2013, 6, 227–235.
[31] Wang, L.; Hu, C.; Shao, L. The [32] antimicrobial activity of nanoparticles: Present situation and prospects for the future. Int. J. Nanomed. 2017, 12, 1227.

تحضير جسيمات الفضة \ ثنائي أوكسيد التيتانيوم لب\قشرة النانوية بواسطة الاستئصال بالليزر وتأثيره كمضاد للبكتيريا

مها طالب توفيق ، فلاح عبد الحسن مطلك

قسم الفيزياء ، كلية العلوم ، جامعة بغداد ، بغداد ، العراق

الملخص

نتيجة لانتشار الأمراض المعدية التي تسببها العديد من البكتيريا الضارة وتطور مقاومة المضادات الحيوية ، يبحث الباحثون وشركات الأدوية عن أدوية جديدة مضادة للبكتيريا. علاوة على ذلك ، نظرًا لارتفاع مساحة سطحها إلى نسبة الحجم (SA: V) والخصائص الفيزيائية والكيميائية الفريدة، تظهر المواد النانوية كعوامل جديدة مضادة للجراثيم في السياق المعاصر. في هذه الدراسة، أظهرنا كيفية صنع NPs TiO_2 /Ag نقية ومستقرة وعالية التركيز. من خلال تسليط ليزر نابض نوع (Nd:YAG)وباطوال موجية مختلفة 1064 نانوميتر وبطول 532 نانوميتر الناتج من التولد التوافقي الثاني باستخدام بلورة KDP وبطول موجي 355 نانوميتر الناتج من التولد التوافقي الثالث باستخدام البلورة اللاخطية KTP على لوحة TiO_2 المغمورة في معلقات الجسيمات النانوية Ag التي تم إنتاجها مسبقًا بطاقات مختلفة تبلغ 200 و 400 و 600 و 800 و 1000 ملي جول، تم إنشاء NPs TiO_2 / Ag. ذروة الامتصاص للعينة التي تم الحصول عليها عند طاقة 1000 ملي جول أكبر من ذروة الامتصاص للعينة المحضرة عند 200 ملي جول ، والتي تُعزى إلى زيادة تركيز الجسيمات النانوية. عند 440 نانومتر ، تكون القمم المتبقية ثابتة تقريبًا. ارتفع الامتصاص عندما انخفض الطول الموجي لليزر من 1064 نانومتر إلى 355 نانومتر وزادت مستويات الطاقة من 200 إلى 1000 ملي جول، وفقًا لنتائجنا. تم اكتشاف أن TiO_2 / Ag له تأثير على النشاط البكتيري ، مع ارتفاع منطقة التثبيط مع زيادة شدة الليزر. أظهرت *E.coli* أنها أكثر مقاومة لـ TiO_2 / Ag من *S.aureus*.